Revista Brasileira de Ensino de Física, vol. 46, e20230297 (2024)
www.scielo.br/rbef
DOI: https://doi.org/10.1590/1806-9126-RBEF-2023-0297

Articles

Revisiting Faraday's Law: A Fresh Perspective Using Neodymium Magnets Moving Under Natural Motion Laws

Um novo olhar à Lei de Faraday: Observando imãs de neodímio sob a ação de leis naturais de movimento

L.V. Montanheiro[*1], F. Tomazi[1], C.A. Dartora[1]

[1]Universidade Federal do Paraná, Departamento de Engenharia Elétrica, Curitiba, PR, Brasil.

Received on October 03, 2023. Revised on May 17, 2024. Accepted on May 22, 2024.

Faraday's law of electromagnetic induction is one of the four Maxwell's equations, presented here in vector notation. Its discovery paved the way for a second industrial revolution based on machines powered by electricity. Roughly speaking, it states that the negative (a Lenz's contribution) of the temporal rate of change of magnetic fields acts as a source for an electric field of rotational nature. In this paper, we discuss readily replicable experiments demonstrating Faraday's law in action, using the motion of a neodymium magnet under three natural motions: i) free fall under gravity; ii) pendular motion under gravity and iii) the magnet placed at the free end of a vibrating ruler. Due to their simplicity, these systems allow for a complete theoretical treatment. We consider more than one way of calculating the induced voltage in a circular coil, by the magnet in motion. This way, students can benefit from the multidisciplinary aspects, connecting the knowledge of kinematics of motion and the electrodynamics of particles in motion. The experimental data was obtained using an oscilloscope and contrasted to the theoretical predictions. In practice, these experiments can be used to estimate the magnetic dipole moment of a permanent magnet.
Keywords: Faraday, neodymium, free-fall, pendulum, vibrations.

A lei de Faraday de indução eletromagnética é uma das quatro equações de Maxwell, apresentada aqui em notação vetorial. Sua descoberta abriu caminho para a segunda revolução industrial baseada em máquinas movidas a eletricidade. De forma geral, a lei afirma que o negativo (uma contribuição de Lenz) da taxa temporal de variação de um campo magnético atua como uma fonte para um campo elétrico de natureza rotacional. Neste artigo, discutimos experimentos facilmente replicáveis que demonstram a lei de Faraday em ação, usando o movimento de um ímã de neodímio sob três ações naturais: i) queda livre sob gravidade; ii) movimento pendular sob gravidade; e iii) o ímã colocado na extremidade livre de uma régua vibrante. Devido à sua simplicidade, esses sistemas permitem um tratamento teórico completo. Consideramos mais de uma maneira de calcular a tensão induzida em uma bobina circular pelo ímã em movimento. Dessa forma, os estudantes podem se beneficiar de aspectos multidisciplinares, conectando o conhecimento da cinemática do movimento e da eletrodinâmica das partículas em movimento. Os dados experimentais foram obtidos usando um osciloscópio e comparados com as previsões teóricas. Na prática, esses experimentos podem ser usados para estimar o momento dipolar magnético de um ímã permanente.
Palavras-chave: Faraday, neodímio, queda-livre, pêndulo, vibrações.

1. Motivation

The authors have observed that post-covid19 quarantined students have struggled with experimental aspects of physics concepts. One might reason this might have been caused by too much of remote and/or virtual laboratory classes. Thus, many students struggle even with reading and operating oscilloscopes in the now live laboratory classes. So, this article is intended to work as a bridge between equations derivations, computer simulations and real world lab-bench measurements. That is the reason schematics, theoretical results, photos and real results have all been shown.

These experiments are readily available as neodymium magnets are ubiquitous and the motions abridged require no extra equipment and even add ease of data interpretation since they will point to the gravitational acceleration constant g or the ruler's elastic constant k. The one key equipment is the oscilloscope which needs to be able to read mere milivoltages.

The work focuses on Faraday's Law, one of the greatest experiments in electromagnetics performed by Michael Faraday, he himself understood to be a skillful experimenter. A very good teaching class introduction to the experiments here proposed would deal with Faraday's hands-on approach to electromagnetics problems and show that experiments are the source of nature's truths.

*Correspondence email address: leciom@ufpr.br

2. Introduction

Electromagnetic phenomena are successfully described by Maxwell's equations, originally proposed by James Clerk Maxwell [1] in the 1861s. Building on previous works by Charles Augustin de Coulomb [2], Hans Christian Oersted [3], Andre Marie Ampére [4], Michael Faraday [5] and Joseph Henry [6], to name a few, Maxwell was able to unite electricity, magnetism and optics in a logical and coherent set of equations. The current form of Maxwell's equations in vector notation is due to Oliver Heaviside [7], which is written in SI units as follows [8–12]:

$$\nabla \cdot \mathbf{D} = \rho, \tag{1}$$

$$\nabla \cdot \mathbf{B} = 0, \tag{2}$$

$$\nabla \times \mathbf{E} = -\frac{\partial \mathbf{B}}{\partial t}, \tag{3}$$

$$\nabla \times \mathbf{H} = \mathbf{J} + \frac{\partial \mathbf{D}}{\partial t}, \tag{4}$$

together with the constitutive relations for material media:

$$\mathbf{D} = \varepsilon_0 \mathbf{E} + \mathbf{P}, \tag{5}$$

$$\mathbf{B} = \mu_0(\mathbf{H} + \mathbf{M}). \tag{6}$$

In the equations, the displacement vector $\mathbf{D}$, the electric field intensity $\mathbf{E}$ and dielectric polarization $\mathbf{P}$ are the electric variables. The magnetic flux density vector $\mathbf{B}$, the magnetic field intensity $\mathbf{H}$ and magnetization $\mathbf{M}$ are the magnetic variables. ε_0 is the vacuum dielectric permittivity and μ_0 is the vacuum magnetic permeability, ρ is the electric charge volumetric density and $\mathbf{J}$ is the electric current density vector.

There is a popular anecdote that Michael Faraday, during a conversation with British Prime Minister William Gladstone, predicted the potential impact of electricity on society and the probable taxation on electric power. When asked by Mr. Gladstone about the usefulness of electricity stuff, Faraday's apocryphal reply was "Why, sir, there is every probability that you will soon be able to tax it!" [13]. Even though there are no reliable sources to confirm the dialogue really happened, Faraday's contributions to electromagnetism and his understanding of the relationship between electricity and society were indeed remarkable. He recognized the transformative potential of his discoveries and played a significant role in the development of electrical technology.

From a technological viewpoint, it was the discovery of the law of electromagnetic induction that allowed a second industrial revolution [14], based on machines powered by electricity. The development and optimization of electrical motors, generators and AC transformers are only possible through the use of Faraday's law. To be fair, the empirical law of electromagnetic induction was discovered independently by the English scientist Michael Faraday in 1831 [15, 16] and the American scientist Joseph Henry in 1832 [17, 18]. The negative sign in the right-hand side of (3) was due to Heinrich Lenz [19], but the mathematical formulation of the law came later, in 1845, through the work of Franz Ernst Neumann [20]. Therefore, it is sometimes referred to as the Faraday-Neumann-Lenz law. The inductance symbol is L, in honor of H. Lenz and it is measured in henries in honor of J. Henry.

In the present contribution, we will focus attention on equation (3), which is known as Faraday's Law of Induction. Going further, the main goal of this paper is to discuss didactic experiments involving Faraday's law effects of permanent magnets under mechanical laws of motion. The magnet to be considered here is a permanent neodymium magnet, which is endowed with a magnetic dipole moment. The mechanical motion laws to which it will be subjected are three: i) free fall under gravity; ii) pendular motion under gravity and iii) the magnet placed at the free end of a vibrating ruler. Due to their simplicity, these systems allow for a complete analytical theoretical treatment. We have described more than one way of calculating the induced voltage in a circular coil by the magnet in motion so that students can benefit from the multidisciplinary aspects, connecting the knowledge of kinematics of motion and electrodynamics of particles in motion. The experimental data can be obtained using an oscilloscope and contrasted to the theoretical predictions. The free-falling magnet experiment was qualitatively discussed in a previous publication at RBEF, by R. Hessel et al. [21].

In this work, the theoretical predictions will be connected to the experimental results in a quantitative way. To do that, the paper is organized as follows: in Section 3, the magnetic potential vector and the corresponding magnetic field created by a magnetic dipole will be deduced from Maxwell's equations in the magnetostatic regime. In Section 4, considering the expressions obtained in Section 3, the induced voltage on a coil by the motion of a permanent magnet will be determined using Faraday's law of induction, as well as from the perspective of Lorentz transformations. Section 5 brings a discussion on the experimental apparatus and the obtained results, which are contrasted to the theoretical expressions deduced in Section 4 for the distinct motions considered. Finally, in Section 8, concluding remarks are added.

3. The Magnetic Field of a Magnetic Dipole

From Maxwell's equations we know that for static fields, electric and magnetic fields become decoupled. Consequently, the field equations describing magnetostatic phenomena are the following [8, 10]:

$$\nabla \cdot \mathbf{B} = 0 \ (2)$$

$$\nabla \times \mathbf{B} = \mu_0 \mathbf{J} + \mu_0 \nabla \times \mathbf{M}, \tag{7}$$

 DOI: https://doi.org/10.1590/1806-9126-RBEF-2023-0297

where the **H** field in the Ampère-Maxwell law, equation (4) was eliminated in favor of **B** through the use of equation (6), $\mathbf{H} = \mathbf{B}/\mu_0 - \mathbf{M}$. In this context **J** represents the current density vector of free electric charges, while $\nabla \times \mathbf{M}$ represents an effective current caused by the magnetization (which can be intrinsic to the medium). Notice that in the static regime the so-called displacement current density vanishes, i.e., $\partial \mathbf{D}/\partial t = 0$.

Equation (2) can be promptly solved using the magnetic potential vector **A**, with **B** defined as follows:

$$\mathbf{B} = \nabla \times \mathbf{A}. \tag{8}$$

It is worth pointing out that only **B** has a physical meaning, therefore the magnetic potential vector **A** is not uniquely defined, since a new potential $\mathbf{A}'$, obtained by adding the gradient of a scalar function f to the original potential, $\mathbf{A}' = \mathbf{A} + \nabla f$, yields the same field **B**. This property is the so-called gauge freedom. It is possible to fix the magnetic potential vector by imposing some gauge fixing conditions. Adopting the Coulomb gauge, $\nabla \cdot \mathbf{A} = 0$, substituting (8) into (7) and using $\nabla \times \nabla \times \mathbf{A} = \nabla(\nabla \cdot \mathbf{A}) - \nabla^2 \mathbf{A}$, we get the Poisson equation:

$$\nabla^2 \mathbf{A}(\mathbf{r}) = -\mu_0 \mathbf{J} - \mu_0 \nabla \times \mathbf{M}, \tag{9}$$

for which a formal solution is given by:

$$\mathbf{A}(\mathbf{r}) = \frac{\mu_0}{4\pi} \iiint_{V'} \frac{[\mathbf{J}(\mathbf{r}') + \nabla' \times \mathbf{M}(\mathbf{r}')]}{|\mathbf{r} - \mathbf{r}'|} d^3\mathbf{r}'. \tag{10}$$

Going further, we are interested in the magnetic field created by a permanent magnet. In the lowest order of approximation, a permanent magnet can be modeled as having a magnetic dipole moment **m** resulting from the alignment of the microscopic spins (and also orbital magnetic moments) of its internal constituents. In this case, we can safely set $\mathbf{J} = 0$ and, assuming the magnet is located at the position $\mathbf{r} = \mathbf{r}_0$ in space, the magnetization is $\mathbf{M}(\mathbf{r}) = \mathbf{m}\,\delta^3(\mathbf{r} - \mathbf{r}_0)$, where $\delta^3(\mathbf{r} - \mathbf{r}_0) = \delta(x - x_0)\delta(y - y_0)\delta(z - z_0)$ is the Dirac delta in 3 spatial dimensions, represented in rectangular coordinates. The reader must be aware of the fact that the product of distributions, like the Dirac delta, is not a distribution in general. In this particular, the product of deltas is not a well-defined delta in the sense of distributions. Such analysis is beyond the scope of the present contribution. We refer the interested reader to Nivaldo A. Lemos, "Convite à Física Matemática" (in Portuguese) (São Paulo, Livraria da Física, 2013) [22] – chapter 9, for more details. We need to calculate the curl of **M**, which acts as a source for the magnetic field. Supposing **m** does not vary w.r.t. (with respect to) **r**, we obtain:

$$\nabla \times \mathbf{M} = \nabla \delta^3(\mathbf{r} - \mathbf{r}_0) \times \mathbf{m}, \tag{11}$$

where the property $\nabla \times (f\mathbf{a}) = \nabla f \times \mathbf{a} + f \nabla \times \mathbf{a}$ was used. Inserting (11) into (10) and performing an integration by parts yields the desired result:

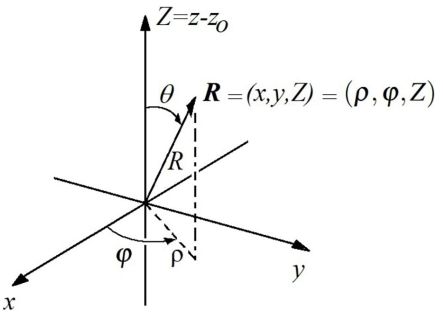

Figure 1: **R** vector in-text mentioned coordinates.

$$\mathbf{A}(\mathbf{r}) = \frac{\mu_0}{4\pi R^3} \mathbf{m} \times \mathbf{R}, \tag{12}$$

where $\mathbf{R} = \mathbf{r} - \mathbf{r}_0$ and $R = |\mathbf{R}|$.

Now consider that the magnetic dipole is oriented along the z-axis, $\mathbf{m} = m\hat{\mathbf{a}}_\mathbf{z}$, and is located at $\mathbf{r_0} = (0, 0, z_0)$. Thus, $\mathbf{R} = (x, y, z - z_0)$, which can be represented in cyllindrical coordinates by (ρ, φ, Z). The modulus of **R** is $R = \sqrt{\rho^2 + Z^2}$, where with $Z = z - z_0 = R\cos\theta$ and $\rho = \sqrt{x^2 + y^2} = R\sin\theta$. For the sake of clarity Figure 1 illustrates the coordinates being used. Due to symmetry considerations, the magnetic potential and magnetic field are not dependent on the azimuthal angle $\varphi = \arctan(x/y)$. In this case, the magnetic potential vector is easily reduced to:

$$\mathbf{A}(\mathbf{r}) = \frac{\mu_0 m}{4\pi R^2} \sin\theta \hat{\mathbf{a}}_\varphi. \tag{13}$$

The magnetic field is promptly obtained by taking the curl of (13) in spherical coordinates (R, θ, φ). The result is [23]:

$$\mathbf{B}(\mathbf{r}) = \frac{\mu_0 m}{4\pi R^3}[2\cos\theta \hat{\mathbf{a}}_\mathbf{r} + \sin\theta \hat{\mathbf{a}}_\theta]. \tag{14}$$

The field lines of a vector field are tangent to the vector itself at each point and can be obtained in the present case by solving the equation $\mathbf{B} \times d\mathbf{l} = 0$, with $d\mathbf{l} = dR\hat{\mathbf{a}}_\mathbf{R} + Rd\theta\hat{\mathbf{a}}_\theta + R\sin\theta d\varphi\hat{\mathbf{a}}_\varphi$ in spherical coordinates. Therefore, for the magnetic dipole field, the resulting equations are $d\varphi = 0$ and $2R\cos\theta d\theta - \sin\theta dR = 0$. The solution for a constant φ is $R(\theta) = R_0 \sin^2\theta$, $0 \leq r_0 < \infty$. These field lines are illustrated in Figure 2. It is worth mentioning that the north and south magnetic poles shown in Figure 2 are a fictitious construction, nevertheless helpful in visualizing the field lines.

4. Faraday-Henry's Law Applied to a Free-Falling Magnet

Consider a permanent magnet, modeled as a magnetic dipole moment $\mathbf{m} = +m\hat{\mathbf{a}}_\mathbf{z}$, initially at rest at some height $z(0) = h_0$ measured from the center of a coil,

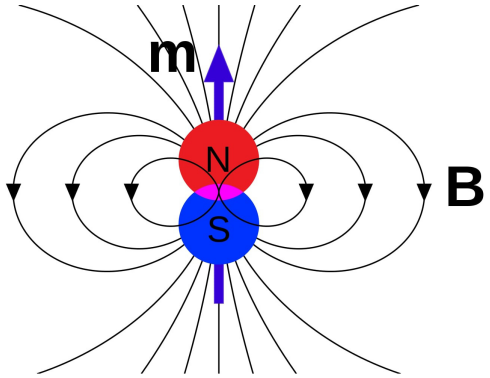

Figure 2: The field lines produced by a magnetic dipole moment $\mathbf{m}$. It is instructive to consider the existence of fictitious north and south poles, with the lines diverging from the north and converging to the south pole, in close analogy to the electric field lines of an electric dipole.

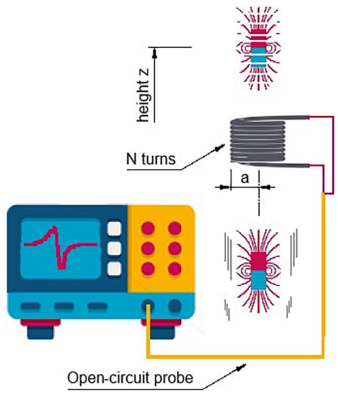

Figure 3: Experimental schematics: A permanent magnet initially at rest is released to move from its initial position $\mathbf{r} = (0, 0, h_0)$, and it can pass through the center of a coil having N turns of radius a. The terminals of the coil are connected to an oscilloscope.

being released to move. The conducting coil has N turns of copper wire, each turn having an averaged radius a. The terminals of the coil are connected to an oscilloscope. Figure 3 illustrates the schematics of the experimental setup.

The free-falling motion of the permanent magnet, assumed to be point-like, is described by $x_0(t) = y_0(t) = 0$ and $z_0(t) = h_0 - gt^2/2$, where $g = 9.81\text{m/s}^2$ is the gravitational acceleration near the Earth's surface. By contrast, in the pendular motion $z_0(t) = h_0 + \Delta h \cos(\omega_0 t - \phi_0)$, where $\Delta h = L\sin(\theta_0)$, being L the length of the ruler and θ_0 the initial angular position of the ruler, ϕ_0 is just an initial phase of the pendular motion. The approximated natural frequency of pendular motion under the influence of gravitational field is given by $\omega_0 = \sqrt{g/L_{ef}}$, where $L_{ef} = \eta L$ is the effective length of the pendulum, which is smaller than true length L by a factor η. It comes from the moment of inertia associated with the mass distribution of the pendulum. For the vibrating ruler scenario we assume a damping factor α and $z_0(t) = h_0 + \Delta h \cos(\omega_0 t - \phi_0)e^{-\alpha t}$, where ω_0 is a natural frequency associated with vibrational modes of the ruler, which has one of its ends fixed, and the other is free to oscillate with amplitude Δh around the average position h_0. Notice that in any of the scenarios, the distance between any point in the coil surface and the permanent magnet is continuously changing. Therefore, the magnetic flux which passes through the coil, defined for any surface S bounded by a closed path C, as follows:

$$\phi_m = \iint_{S(C)} \mathbf{B}\cdot d\mathbf{a} = \oint_C \mathbf{A}\cdot d\mathbf{l}, \tag{15}$$

is a time-varying quantity. Faraday's law states that the electromotive force (or induced voltage V_{ind} along a closed path) is equal to the negative of the time derivative of the magnetic flux enclosed by the path, i.e.:

$$V_{ind} = \oint_C \mathbf{E}\cdot d\mathbf{l} = -\frac{d\phi_m}{dt}. \tag{16}$$

The orientation of the surface vector corresponding to the oriented surface $\mathbf{S} = \int_{S(C)} d\mathbf{a}$ is defined by the orientation of the closed path C, using the right-hand rule. Notice that equation (16) is the integral version of (3). To arrive at the integral version we need to integrate the differential form of Faraday's law w.r.t. an area S, and then apply Stokes's theorem:

$$\iint_{S(C)} \nabla\times\mathbf{E}\cdot d\mathbf{a} = \oint_C \mathbf{E}\cdot d\mathbf{l} = -\iint_{S(C)} \frac{\partial\mathbf{B}}{\partial t}\cdot d\mathbf{a}. \tag{17}$$

As a last step, assume the modulus $S(C)$ and the orientation of the coil do not change in time, for the sake of simplicity. So much so that the partial derivative w.r.t. time can be pulled outside the integral, becoming a total derivative. As a matter of fact, a careful analysis shows that for the more general case where the surface changes in time, we have:

$$\oint_C \mathbf{E}\cdot d\mathbf{l} = -\frac{d\phi_m}{dt} = -\iint_{S(C)} \frac{\partial\mathbf{B}}{\partial t}\cdot d\mathbf{a} + \oint_C \mathbf{v}\times\mathbf{B}\cdot d\mathbf{l}, \tag{18}$$

which gives the same answer as (17), provided that we redefine the electric field to $\mathbf{E}' = \mathbf{E} - \mathbf{v}\times\mathbf{B}$. A more detailed discussion is presented by A. Feoli et al. [24].

Going further, we need to calculate the magnetic flux passing through the coil, due to the magnetic field created by the permanent magnet instantaneously. Suppose the permanent magnet is located at the origin of the coordinate system (x, y, Z), i.e., $x = y = 0$ and $Z = z - z_0 = 0 \to z = z_0$, and the surface vector of the coil, which will define the closed path of interest here, is colinear to the magnetic dipole moment, itself assumed to be aligned with the z-axis. Additionally, considering (14) when obtaining the magnetic flux first

 DOI: https://doi.org/10.1590/1806-9126-RBEF-2023-0297

we need to calculate the projection of the magnetic field onto the z-axis, i.e., $\mathbf{B}\cdot\hat{\mathbf{a}}_\mathbf{z}$:

$$\mathbf{B}\cdot\hat{\mathbf{a}}_\mathbf{z} = \frac{\mu_0 m}{4\pi R^3}[2\cos\theta\hat{\mathbf{a}}_\mathbf{R}\cdot\hat{\mathbf{a}}_\mathbf{z} + \sin\theta\hat{\mathbf{a}}_\theta\cdot\hat{\mathbf{a}}_\mathbf{z}]. \quad (19)$$

The unit vector $\hat{\mathbf{a}}_\mathbf{z}$ of the cartesian (or cylindrical) coordinate system can be expressed in terms of spherical basis vectors, as follows:

$$\hat{\mathbf{a}}_\mathbf{z} = \cos\theta\hat{\mathbf{a}}_\mathbf{R} - \sin\theta\hat{\mathbf{a}}_\theta. \quad (20)$$

Substituting (20) into (19) and performing the scalar products we obtain:

$$\mathbf{B}\cdot\hat{\mathbf{a}}_\mathbf{z} = \frac{\mu_0 m}{4\pi R^3}[2\cos^2\theta - \sin^2\theta] = \frac{\mu_0 m}{4\pi R^3}[3\cos^2\theta - 1]. \quad (21)$$

From the geometry of the problem, for any point (ρ,φ,z) located at the surface of the coil, delimited by the coil perimeter we have $\cos\theta = Z/R$, $\sin\theta = \rho/R$, with $R=\sqrt{\rho^2+Z^2}$ and $Z = z - z_0$. Remembering that the permanent magnet is located instantaneously at $(0,0,z_0)$ and assuming the coil to be located at the plane $z=0$, we have for the magnet velocity $v_z = \dot{z}_0 = -dZ/dt$.

The magnetic flux through the coil, assuming the area of the coil is oriented parallel to the magnetic dipole moment of the permanent magnet, is given by:

$$\begin{aligned}\phi_m &= \iint_{S(C)}\mathbf{B}\cdot d\mathbf{a} = \int_{\rho=0}^{a}\int_{\varphi=0}^{2\pi}\mathbf{B}\cdot\hat{\mathbf{a}}_\mathbf{z}\rho d\rho d\varphi \\ &= \frac{\mu_0 m}{4\pi}\int_{\rho=0}^{a}\int_{\varphi=0}^{2\pi}\frac{1}{R^3}[3\cos^2\theta-1]\rho d\rho d\varphi \\ &= \frac{\mu_0 m}{2}\int_{\rho=0}^{a}\left[\frac{3Z^2}{(\rho^2+Z^2)^{5/2}} - \frac{1}{(\rho^2+Z^2)^{3/2}}1\right]\rho d\rho. \end{aligned} \quad (22)$$

As a final step to integrate (22) and obtain the desired result we perform a change of variables, $u=\rho^2+Z^2$ and $du = 2\rho d\rho$. After a straightforward calculation we get:

$$\phi_m = \frac{\mu_0 m a^2}{2(a^2+Z^2)^{3/2}}. \quad (23)$$

Now the induced voltage in the N-turn coil is given by Faraday's law:

$$V_{ind} = -N\frac{d\phi_m}{dt} = -N\frac{d\phi_m}{dZ}\dot{Z}. \quad (24)$$

Notice that the total induced voltage in the coil corresponds to the sum of the induced voltage in each of the N turns. Assuming that the turns are located at nearly the same height $z=0$ and have the same radius a, it leads to multiplying the induced voltage induced on a single turn by N. The desired result is:

$$V_{ind} = -\frac{3\mu_0 m N a^2}{2}\frac{Z\dot{Z}}{(a^2+Z^2)^{5/2}}, \quad (25)$$

with $Z = z - z_0(t)$ and $\dot{Z} = -\dot{z}_0$.

Now it is important to discuss the sign of the induced voltage. For the sake of simplicity we will discuss the case of a free-falling magnet. Assume the magnetic dipole moment points upwards respective to the z-axis, i.e., $\mathbf{m} = +m\hat{\mathbf{a}}_\mathbf{z}$ and it is located at the origin of the coordinate system. Therefore, the component of the magnetic field along the z axis is also pointing upwards. If we assume the oriented surface of the coil also points towards $+\hat{\mathbf{a}}_\mathbf{z}$, it means that the closed path C in Faraday's law must be traveled counterclockwise, as seen by an observer above the coil, looking downwards at the coil. Thus, the calculated magnetic flux enclosed by the coil is always positive, but its magnitude changes during the free fall of the magnet. Initially the magnetic flux increases due to the decrease in the distance between the coil and the permanent magnet. Remember that the magnetic field produced by a magnetic dipole depends on $1/r^3$. The maximum magnetic flux occurs when the magnet is passing through the center of the coil. After that point, for which $h_0 = gt^2/2$, the magnetic flux decreases again. The induced voltage is given by $V_{ind} = -d\phi_m/dt$, meaning that at the terminals of the coil, the induced voltage becomes negative while the magnetic flux is increasing, it reaches a minimum and then starts to increase, until a maximum is reached. After a while, the permanent magnet will be far from the coil and magnetic flux as well as its derivative will be negligible, leading to $V_{int}=0$ again. If the magnetic dipole is oriented in the negative sense of the z-axis or the reference terminal for the oscilloscope probe is reversed, it reverses the sign of V_{ind} being measured.

4.1. Analysis using the magnetic potential vector

A distinct approach to calculating the induced voltage V_{ind} is through the use of electromagnetic potentials. The electric and magnetic fields, $\mathbf{E}$ and $\mathbf{B}$, respectively, are obtained from the electromagnetic potentials ϕ and $\mathbf{A}$, as follows:

$$\begin{aligned}\mathbf{E} &= -\nabla\phi - \frac{\partial\mathbf{A}}{\partial t}, \quad (26)\\ \mathbf{B} &= \nabla\times\mathbf{A}. \quad (8)\end{aligned}$$

In our previous calculation, the magnetic field $\mathbf{B}$ was already obtained from (8). Using gauge freedom we can set the scalar potential ϕ to zero. Thus, the electric field $\mathbf{E}$ produced by the free-falling magnet is given by:

$$\begin{aligned}\mathbf{E} &= -\frac{\partial\mathbf{A}}{\partial t} = -\frac{\mu_0 m}{4\pi}\frac{d}{dt}\frac{\sin\theta}{R^2}\hat{\mathbf{a}}_\varphi \\ &= -\frac{\mu_0 m}{4\pi R^3}[R\dot{\theta}\cos\theta - 2\dot{R}\sin\theta]\ \hat{\mathbf{a}}_\varphi, \end{aligned} \quad (27)$$

where the expression for the vector $\mathbf{A}$ was previously written in equation (13). Notice that the electric field $\mathbf{E}$ exists independently of the presence of a conducting coil. Going further, we are interested in the voltage induced

in the coil terminals, as a result of the electric force exerted by the electric field $\mathbf{E}$ on the free charge carriers of the conducting wires. Since the coil has a fixed radius $\rho = a$ we have $\cos\theta = Z/r$ and $\sin\theta = a/r$, with $r = \sqrt{a^2 + Z^2}$. The electromotive force becomes then,

$$V_{ind} = \oint_C \mathbf{E} \cdot d\mathbf{l} = -\frac{\mu_0 mNa}{2R^3}[R\dot{\theta}\cos\theta - 2\dot{R}\sin\theta], \quad (28)$$

where we have used $d\mathbf{l} = ad\varphi\hat{\mathbf{a}}_\varphi$, and the integral produces a factor of $2\pi a$ times the electric field component E_φ. Now we want to express $\dot{R}$ and $\dot{\theta}$ in terms of $\dot{Z}$, i.e.:

$$\dot{R} = \frac{dR}{dZ}\dot{Z} = \frac{Z\dot{Z}}{R}, \quad (29)$$

$$\dot{\theta} = \frac{d\theta}{dZ}\dot{Z} = -\frac{a\dot{Z}}{R^2}. \quad (30)$$

To calculate $d\theta/dZ$ with $\theta = \arctan(a/Z)$ the following derivative is helpful:

$$\frac{d}{dx}\arctan(x) = \frac{1}{1+x^2}. \quad (31)$$

The intermediate steps are left as an exercise, being the desired result

$$R\dot{\theta}\cos\theta - 2\dot{R}\sin\theta = -\frac{3aZ\dot{Z}}{R^2} \quad (32)$$

Finally, replacing (32) into (28) we arrive at the same result as (25).

4.2. The Lorentz transformations viewpoint

An alternative viewpoint is to consider a Lorentz transformation from the permanent magnet rest frame to the coil reference frame. In the magnet frame there is only a magnetostatic field $\mathbf{B}$ produced by the magnetic dipole, while in the coil reference frame, the magnet is moving. The Lorentz transformations for the electromagnetic fields, in SI units, are given by [8]:

$$\mathbf{E}' = \gamma(\mathbf{E} + \mathbf{v}\times\mathbf{B}) - \frac{\gamma^2}{\gamma+1}\frac{\mathbf{v}}{c}\left(\frac{\mathbf{v}}{c}\cdot\mathbf{E}\right), \quad (33)$$

$$\mathbf{B}' = \gamma\left(\mathbf{B} - \frac{\mathbf{v}}{c^2}\times\mathbf{E}\right) - \frac{\gamma^2}{\gamma+1}\frac{\mathbf{v}}{c}\left(\frac{\mathbf{v}}{c}\cdot\mathbf{B}\right), \quad (34)$$

where $\mathbf{E}$ and $\mathbf{B}$ are the electromagnetic fields in one inertial reference frame and $\mathbf{E}'$ and $\mathbf{B}'$ are the field in another inertial frame moving with velocity $\mathbf{v} = \dot{z}_0\hat{\mathbf{a}}_\mathbf{z} = -\dot{Z}\hat{\mathbf{a}}_\mathbf{z}$ w.r.t. the unprimed frame, $\gamma = 1/\sqrt{1-(v/c)^2}$ is the Lorentz factor and c is the speed of light in vacuum.

As a matter of fact, the reference frame of the magnet in motion in the cases under consideration, is not truly inertial. Nevertheless, the motion takes place at a relative speed $v << c$, therefore we can attribute an instantaneous Lorentz frame to the moving magnet in the coil reference frame. Also notice that $v/c << 1$ and $\gamma \approx 1$. And so we get:

$$\mathbf{E}' \approx \mathbf{v}\times\mathbf{B} = -\frac{\mu_0 m}{4\pi R^3}\dot{Z}\hat{\mathbf{a}}_\mathbf{z}\times[2\cos\theta\hat{\mathbf{a}}_\mathbf{r} + \sin\theta\hat{\mathbf{a}}_\theta], \quad (35)$$

$$\mathbf{B}' \approx \mathbf{B}. \quad (36)$$

Making use of $\hat{\mathbf{a}}_\mathbf{z} = \cos\theta\hat{\mathbf{a}}_\mathbf{r} - \sin\theta\hat{\mathbf{a}}_\theta$ yields:

$$\mathbf{E}' \approx \mathbf{v}\times\mathbf{B} = -3\frac{\mu_0 m}{4\pi R^3}\dot{Z}\sin\theta\cos\theta\hat{\mathbf{a}}_\varphi = -3\frac{\mu_0 maZ\dot{Z}}{4\pi R^5}\hat{\mathbf{a}}_\varphi, \quad (37)$$

which coincides with (27). It is important to mention that it is perfectly possible to consider more general transformations when one reference frame is accelerated w.r.t. the other. These are known as Rindler transformations [25]. Rindler transformations were used in Goto [26] to obtain the electromagnetic fields of free-falling charge in a uniform gravitational field. The fields obtained in the accelerated regime are quite different from those obtained at constant velocity even in the regime $v << c$. It is an important issue when discussing the radiation emitted by free-falling charges under the perspective of general relativity. Notice that from Maxwell's equations considered in Lorentz frames, accelerated charges must radiate, but the discussion under the perspective of general relativity is beyond the scope of the present paper. Here, it is the free fall of a magnetic dipole that is under analysis. Lorentz transformations and Rindler transformations yield similar results provided that the condition $gt << c$ is satisfied.

5. The Free-Falling Magnet Experimental Results

The experiment was performed in the Magnetic Measurements ans Instrumentation Laboratory (LAMMI) of the Federal University of Paraná (UFPR), using very simple instrumentation found at any undergrad laboratory of Physics or Electrical Engineering courses. Basically, it consisted of an oscilloscope, enameled copper wire for making the coil, which is wound onto a 20 cm long and 3.2 cm in diameter PVC water pipe. The pipe serves only as a guide for the permanent magnet and a supporter for the coil. A neodymium magnet (NdFeB) was selected for the experiment, since it has a high magnetic dipole moment, enhancing the induced voltage

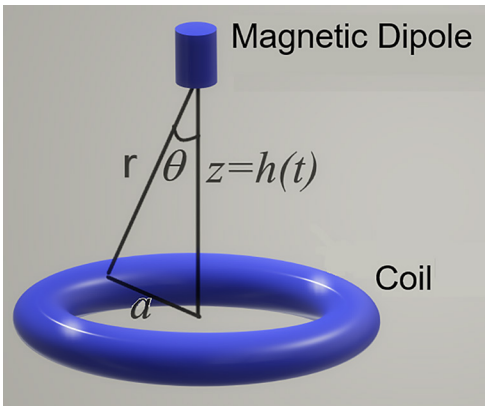

Figure 4: Schematics of the magnet in free-fall motion experiment.

 DOI: https://doi.org/10.1590/1806-9126-RBEF-2023-0297

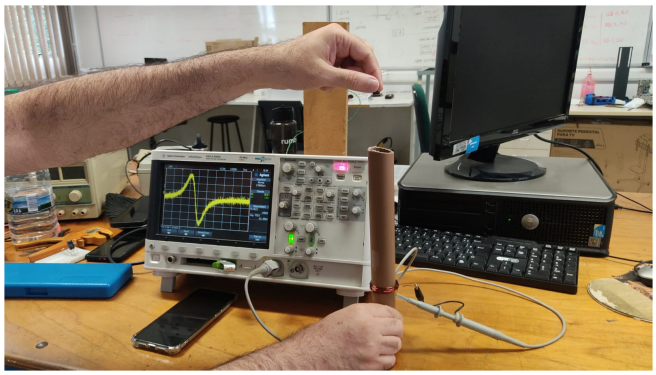

Figure 5: Experimental setup: A permanent magnet initially at rest is released to free fall from height $h_0 = 30$ cm, and it passes through the center of a coil having $N = 30$ turns of radius $a = 1.5$ cm. The terminals of the coil are connected to an oscilloscope Agilent DSOX 2002A.

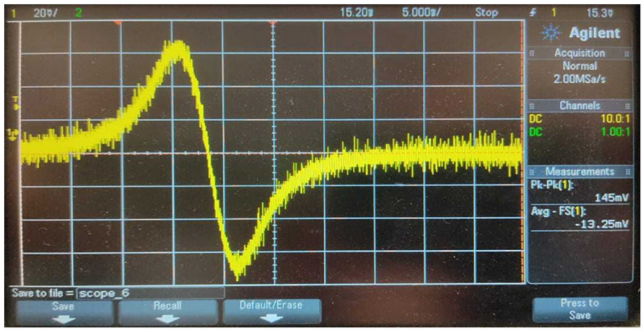

Figure 6: Magnification of the oscilloscope screen for a permanent magnet free-falling experiment.

signal, but any other permanent magnet could be chosen. An schematic is available on Figure 4.

Specifically, we fabricated the coil with an AWG 24 copper wire, having $N = 30$ turns, The radius of the coil was $a = 1.5$ cm, being fixed by the PVC pipe. The oscilloscope we used was an Agilent model DSO-X 2002A. The experimental setup is illustrated in Figure 5. The permanent magnet was released from a height $h_0 \approx 40$ cm from the coil center.

A magnification of the oscilloscope screen is shown in Figure 6. It is important to mention that the oscilloscope must be operated in the single-run mode, i.e., it displays a single measurement after the trigger is fired. Therefore, the trigger level must be reasonably adjusted to obtain a clean measurement. In our experiment, the trigger level was set around 15 mV in the rising mode. The peak voltage was around 60 mV, so we set 20 mV per division, while the time scale was set to 5 ms per division. Notice that the total time of flight for a particle in free fall from a height of $\Delta h \sim 40$ cm is in the range of $t = \sqrt{2\Delta h/g} \sim 285$ ms. So, it is expected that the induced voltage in the coil will have a duration $\Delta t < 285$ ms, typically. Indeed, it can be observed on the screen of the oscilloscope.

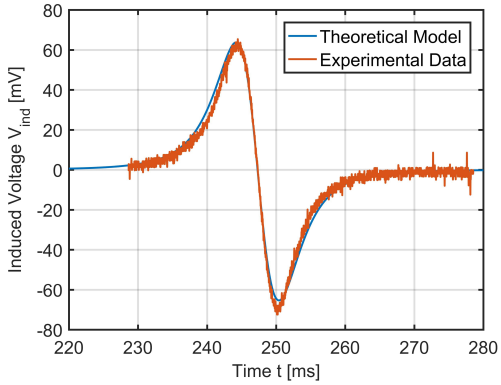

Figure 7: A comparison between the experimental data collected from a free-falling neodymium magnet from an initial height $h_0 = 40$ cm, passing through the center of a coil with $a = 1.5$cm and $N = 30$ turns, and the theoretical prediction from equation (25).

The measurement at the coil's terminals must be performed in an open circuit configuration, to ensure that the induced voltage is really being measured. This way, the oscilloscope probes must be set to high impedance (1 MOhm). One of the terminals of the coil is connected to the probe measurement tip and the other to the GND (ground). Of course, if high-impedance ports are not available in the oscilloscope, a high input impedance buffer with unitary gain, built using a common operational amplifier can be easily constructed.

The modern-day oscilloscope allows to save the experimental data in .CSV or .DAT archives, but for old equipment, if electronic data saving is not available it is possible to take a photograph of the oscilloscope screen and then use one of the many graphical data extractors at disposal for free on the web.

Notice the raw data has high-frequency noise, which can be eliminated through low-pass filters. A comparison between our experimental data and the theoretical equation (25) is shown in Figure 7. As can be seen, the experimental data is in agreement with the predictions from the theory, which is confirmed by the similar shapes, time duration of the pulses and amplitudes of the curves. It is worth mentioning that usually some time translation and vertical shift must be applied to the data collected from the oscilloscope. The magnetic dipole moment of the magnet is used as a fitting parameter. We found it to be $m = 0.37$ A.m^2 in our experiment. Supposing one Bohr magneton $\mu_B = 9.27 \times 10^{-24}$ A.m^2 per atom and $n = 5 \times 10^2 8$ atoms/m^3 in the magnet, for a magnet with volume $V = 0.8$ cm^3 we estimate that $m = \mu_B n V \approx 0.37$ A.m^2, which is in agreement with the value obtained from the fitting.

Numerical integration of experimental data for V_{ind} yields the magnetic flux $N\phi_m = -\int^t V_{ind} dt'$. Notice that the integration acts as a low-pass filter. The experimentally obtained magnetic flux is then compared

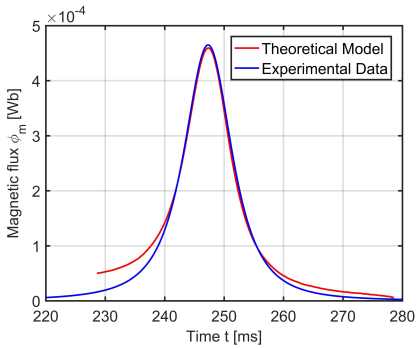

Figure 8: Comparison between the experimental results for the magnetic flux enclosed by the N-turn coil, obtained numerically integrating the experimental data, and the theoretical prediction from equation (23).

to the theoretical prediction, which is given by N times the magnetic flux of a single turn, calculated through equation (23). The comparison is illustrated in Figure 8, with good agreement.

6. The Magnet in Pendular Motion Experiment

The schematics of the proposed experiment is illustrated in Figure 9. A permanent magnet is placed at the free

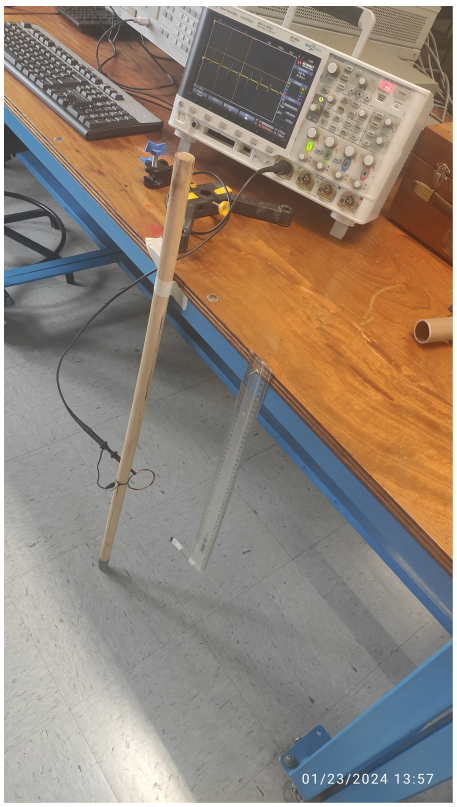

Figure 9: Photo of the experimental setup for the magnet in pendular motion.

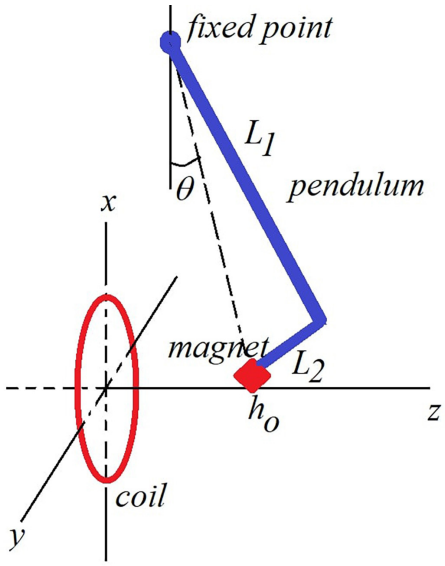

Figure 10: Schematics of the magnet in pendular motion experiment.

end of an L-shaped pendulum, with $L_1 > L2$. The magnetic moment of the magnet is oriented along the z-axis, being colinear to the surface vector of the N-turn coil. A photo of the setup can be seen on Figure 10.

Assuming $L_1 >> L_2$, the angle θ is given approximately by the line L_1 of the pendulum and the x-axis. Suppose the total mass of the pendulum is homogeneously distributed, we can apply Newton's second law for angular momentum. For a mass Δm at a distance r from the fixed point, it reads:

$$I\frac{d^2\theta}{dt^2} = -\Delta mgr\sin\theta, \tag{38}$$

being $I = \Delta mr^2$ the moment of inertia for the infinitesimal mass Δm in the pendulum. Integrating both sides with respect to r, from 0 to L_1 and neglecting the contribution of L_2, for small values of $\sin\theta \approx \theta$ we get:

$$\frac{d^2\theta}{dt^2} = -\omega_0^2\theta, \tag{39}$$

where $\omega_0 = s\sqrt{g/L_{ef}}$ and $L_{ef} = 2L_1/3$. Corrections to the L_{ef} are expected, coming from the segment L_2 and the magnet mass. Considering θ_0 as the maximum angle the pendulum acquires with respect to the x-axis and ϕ_0 an initial phase, the solution of the above equation will be:

$$\theta(t) = \theta_0\cos(\omega_0 t - \phi_0). \tag{40}$$

Now, neglecting small changes of x for the magnet placed at the tip of L_2, we get the component $z_0(t)$ of the magnet position vector:

$$z_0(t) = h_0 + L_1\sin[\theta(t)] \approx h_0 + L_1\theta_0\cos(\omega_0 t - \phi_0). \tag{41}$$

 DOI: https://doi.org/10.1590/1806-9126-RBEF-2023-0297

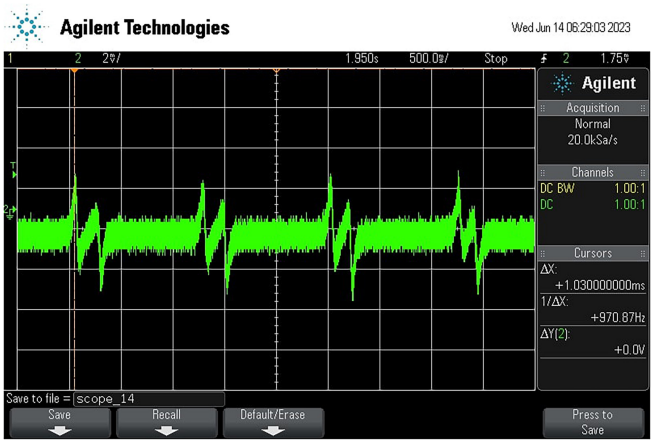

Figure 11: Typical result for the pendulum experiment displayed on the oscilloscope screen.

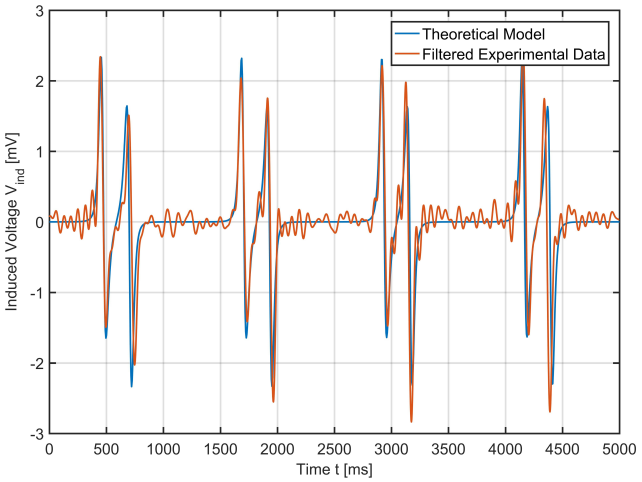

Figure 12: Comparison between the theory and experiment for the coil's induced voltage in the pendular motion experiment.

Notice that in practice there are friction forces leading to a damping factor for the pendulum motion, which can be modeled by multiplication of $\theta(t)$ by a factor $e^{-\alpha t}$. However, for the time scale of a few cycles of the pendular motion in the experiment we conducted, it was verified that the damping effect is negligible. In this context the velocity $v(t) = dZ/dt = -\dot{z}_0(t)$ will be given by:

$$\dot{Z} = v(t) = \omega_0 L_1 \theta_0 \sin(\omega_0 t - \phi_0). \tag{42}$$

Now, the theoretical results are obtained by substitution of (41) and (42) into equations (22) and (25), for the magnetic flux enclosed by the coil at $z = 0$ and the induced voltage at the coil. The parameters we used in the experiment are the following: a coil having radius $a = 1.85$ cm and $N = 30$ turns, a neodymium permanent magnet with $m \approx 0.1$ A.m^2, and a pendulum made using an acrylic ruler, with $L_1 = 50$ cm, and an acrylic cylinder of diameter ~ 7 mm and length $L_2 = 7$ cm. Notice that $L = \sqrt{L_1^2 + L_2^2} = 50.48\text{cm} \approx L_1$. The initial distance was $h_0 = 13$ cm and $\theta_0 \approx 18^o$. The values of ω_0 and ϕ_0 were adjusted for the best fitting of the experimental data. A typical result displayed on the oscilloscope screen is shown in Figure 11. Notice that the result has a high-frequency noise.

After saving the experimental data into a .CSV file, we mathematically applied a low-pass filter to remove the high-frequency noise. It was done by calculating numerically the Fourier transform of the raw experimental data for the induced voltage, $V_{exp}(t)$, as follows:

$$\tilde{V}_{exp}(\omega) = \int_{-\infty}^{\infty} V_{exp}(t) e^{-i\omega t} dt, \tag{43}$$

where the limits of the integral are the initial and final time of the acquired data, in practice. Next we applied a low-pass filter with ideal transfer function $\tilde{G}(\omega)$:

$$\tilde{G}(\omega) = \begin{cases} 1, & |\omega| < 20\omega_0, \\ 0, & |\omega| \geq 20\omega_0. \end{cases} \tag{44}$$

It is worth mentioning that the filter must be adjusted case by case, to remove the high-frequency noise while still reproducing the experimental result. The filtered experimental data will be given by numerically calculated inverse Fourier transform of $\tilde{G}(\omega)\tilde{V}_{exp}(\omega)$:

$$V_{exp}(t) = \frac{1}{2\pi} \int_{-\infty}^{\infty} \tilde{G}(\omega)\tilde{V}_{exp}(\omega) e^{i\omega t} d\omega. \tag{45}$$

The comparison between the filtered experimental data and the theoretical results obtained combining equations (41), (42) and (25) is illustrated in Figure 12. The best fitting was obtained by making $\omega_0 = 5.1069$ rad/s, which leads to an effective length $L_{ef} \approx 37.6$ cm, corresponding to $\eta = 0.7523$, which is $\sim 13\%$ higher than the approximate value of $2L_1/3$. The initial phase was $\phi_0 = -8^o$. The agreement is quite good.

Figure 13 shows a comparison between the magnetic flux obtained from numerical integration of $V_{exp}(t)$

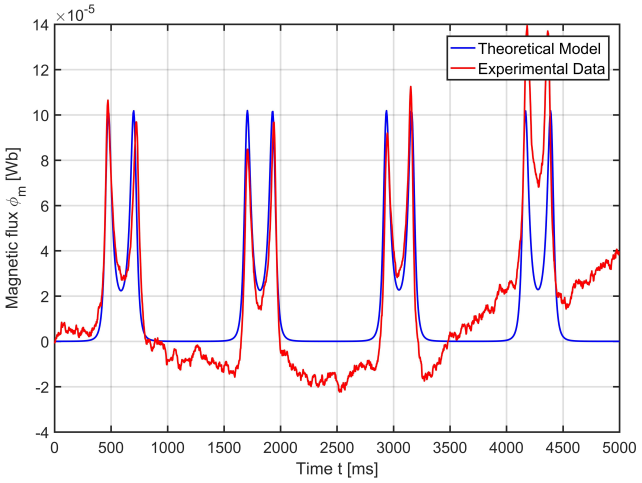

Figure 13: Comparison between the theory and experiment for the magnetic flux enclosed by the coil in the experiment of a magnet displaying a pendular motion.

and the theoretical results obtained combining equations (41), (42) and (22). Despite the low-frequency noise in the measured voltage and a small offset, the curves qualitatively coincide in shape and periodicity.

7. The Magnet Attached to a Vibrating Ruler

The next experiment could be used as an extractor for the vibrational modes of a rod (or in our case an acrylic ruler) with one of its ends fixed and the other free to oscillate around the equilibrium point. The setup is illustrated in Figure 14. A photo can be seen on Figure 15

A permanent magnet is attached to the free end of the ruler, above a coil which is a distance h_0 from the equilibrium position of the ruler's end. An initial displacement Δh from the equilibrium position is applied and the ruler's end will oscillate around the equilibrium, with natural frequency ω_0, which is strongly dependent on the ruler's length. In this experiment the damping effect clearly manifests in the time window we captured in the oscilloscope screen. Therefore, approximate expressions for the magnet motion are as follows:

$$z_0(t) = h_0 + \Delta h \cos(\omega_0 t - \phi_0) e^{-\alpha t}, \tag{46}$$

$$\dot{Z} = -\dot{z}_0 = \Delta h[\omega_0 \sin(\omega_0 t - \phi_0) + \alpha \cos(\omega_0 t - \phi_0)] e^{-\alpha t}. \tag{47}$$

In a typical experiment we set the following parameters: magnetic dipole moment $m = 0.37$ A.m^2, a coil with 30 turns and radius $a = 1.85$ cm, $h_0 = 2.55$ cm and a ruler with $L = 20$ cm from the free to the fixed end. The parameters Δh, ω_0 and ϕ_0 were varied to obtain the best fitting. Figure 16 illustrates a typical experimental result for the voltage induced on the coil, including the noise.

We notice the periodic behavior, compatible with a vibrating magnet near the coil, but there is also a background noise which we aim to remove. The damping is also clearly present. Regardless, we perform a numerical Fourier transform of the data displayed in Figure 16, to obtain the spectrum $\tilde{V}_{exp}(\omega)$. It allows one to identify the frequency ω_0 of the vibrating magnet, as well as to determine the cutoff frequency of an ideal low-pass filter, used to remove the high-frequency noise. The absolute value of the spectrum is shown in Figure 17.

From Figure 17, we determined that $\omega_0 = 59$ rad/s, which is closer to the correct value than measuring the period of oscillation T in Figure 16 and then obtain

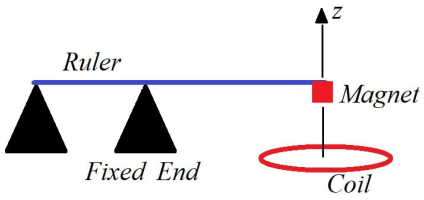

Figure 14: Experimental setup for the vibrating ruler. One of the ruler's ends remains fixed while the other is free to vibrate. The magnet is attached to the free end, above a coil, which will detect an induced voltage produced by the excited vibrating modes.

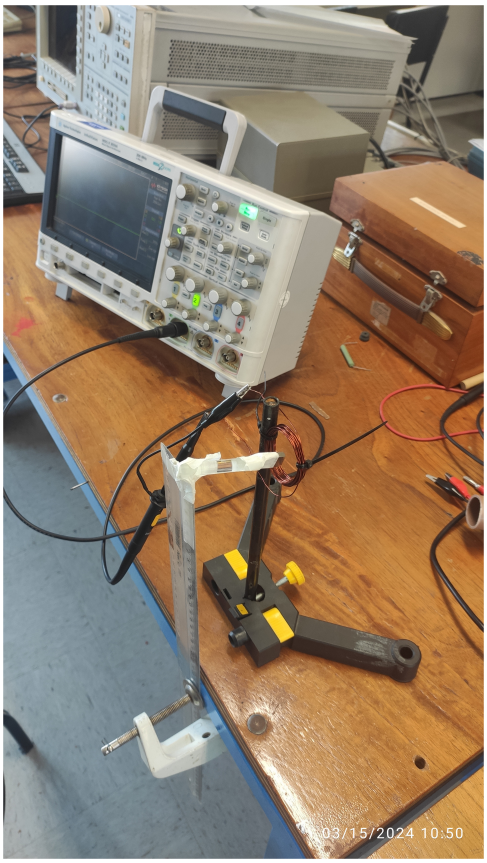

Figure 15: Photo of the experimental setup for the magnet in vibrating motion.

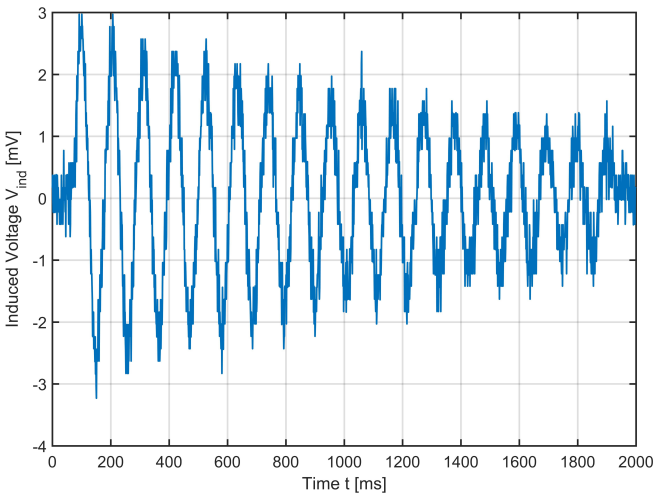

Figure 16: Typical measured result for the induced voltage in the vibrating ruler experiment.

 DOI: https://doi.org/10.1590/1806-9126-RBEF-2023-0297

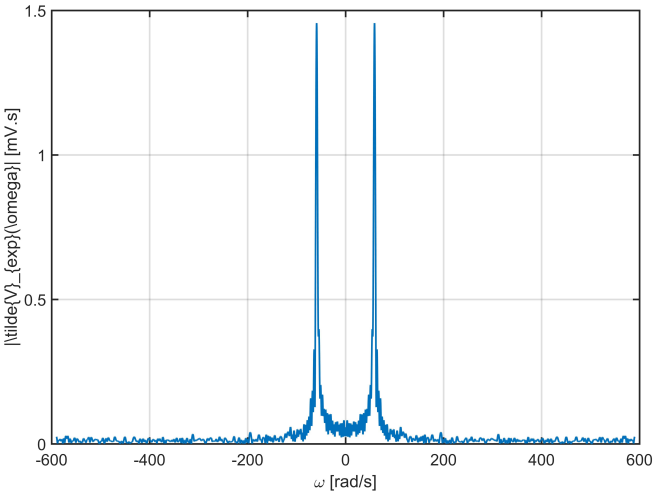

Figure 17: The spectral function $\tilde{V}_{exp}(\omega)$ for a typical measurement in the vibrating ruler experiment.

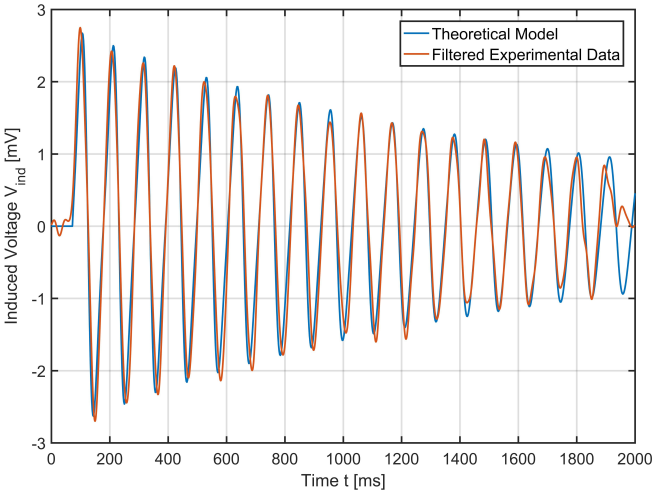

Figure 18: A comparison of the induced voltage in the coil between the induced voltage filtered experimental data and the theoretical predictions obtained inserting the equations of motion (46) and (47) into (25). The parameters of the vibrating magnet are $\omega_0 = 59$ rad/s, $\Delta h = 0.7$ cm, $\alpha = 0.5$ s^{-1} and $\phi_0 = 243.4^o$.

$\omega_0 = 2\pi/T$, due to the noise present in the raw data. We also set the low-pass filter cutoff frequency to be $4\omega_0$. The theoretical curves for induced voltage and magnetic flux were obtained by inserting the equations of motion (46) and (47) into (25) and (23). The obtained results are shown in Figures 18 and 19. The best fitting was obtained by setting $\Delta h = 0.7$ cm, $\alpha = 0.5$ s^{-1} and $\phi_0 = 243.4^o$.

8. Conclusion

In this paper, we have discussed in detail the realization of didactical experiments demonstrating Faraday's law. They consisted of the motion of a permanent magnet

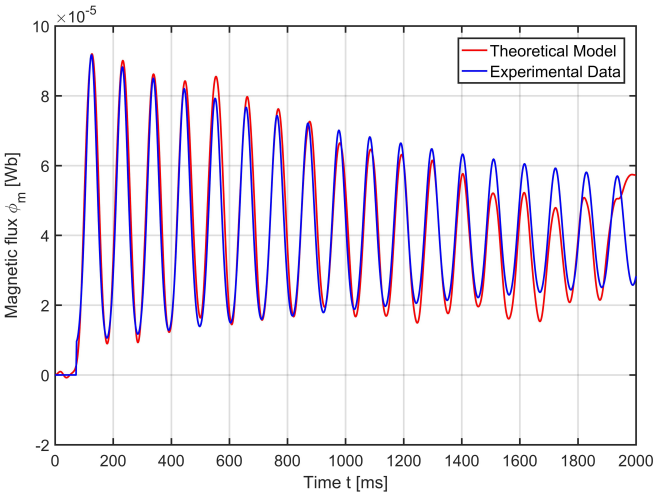

Figure 19: Comparison between theory and experiment for the magnetic flux enclosed by the coil in the vibrating ruler experiment.

in three scenarios: i) free-fall of a magnet under the gravitational influence, passing through the center of a conducting coil, whose terminals were connected to an oscilloscope; ii) the pendular motion of a magnet placed at the free end of a pendulum, and iii) the magnet attached to the end of an acrylic ruler. Theoretical calculations concerning the voltage induced through the coil were performed using three distinct routes: i) directly determining the magnetic flux produced by the free-falling magnet enclosed by the coil; ii) using the electromagnetic potentials to obtain the electric field and then the induced voltage along the closed path where the coil is placed and iii) by means of reference frame Lorentz transformations in the limit of $v << c$. Due to its simplicity, such a complete theoretical treatment was taken into account. The data obtained from the experimental realization quantitatively agree with the theoretical predictions. The fitting allowed us to estimate the magnetic dipole moment of the permanent magnet used in the experiment, or the vibrating frequency of the ruler, for example.

Acknowledgments

C.A. Dartora wishes to acknowledge the support of CNPq – [Brazilian] National Research Council for the support in shape of a Productivity Research Grant.

References

[1] B. Mahon, *The man who changed everything: the life of James Clerk Maxwell* (John Wiley & Sons, New Jersey, 2004).

[2] C.A. Coulomb, *Coulomb and the evolution of physics and engineering in eighteenth-century France* (Princeton University Press, Princeton, 1971).

[3] D.C. Christensen, *Hans Christian Ørsted: reading nature's mind* (Oxford University Press, Oxford, 2013).
[4] A.K.T. Assis and J. Chaib, *Eletrodinâmica de Ampère* (Editora da Unicamp, Campinas (2011)).
[5] A. Hirshfeld, *The electric life of Michael Faraday* (Bloomsbury Publishing, New York, 2009).
[6] A.E. Moyer, *Joseph Henry* (Smithsonian Books, Washington, 2018).
[7] B. Mahon, *Oliver Heaviside: maverick mastermind of electricity* (Institution of Engineering and Technology, London, 2009).
[8] J.D. Jackson, *Classical electrodynamics* (John Wiley & Sons, New Jersey, 2021).
[9] M.N.O. Sadiku, *Elements of Electromagnetics* (Oxford University Press, Oxford, 2010).
[10] J.R. Reitz, *Foundations of electromagnetic theory* (Pearson Education India, Tamil Nadu, 2009).
[11] D.J. Griffiths and R. College, *Introduction to Electrodynamics* (Prentice Hall of India, New Delhi, 1998), v. 3.
[12] C.A. Dartora, *Teoria do campo eletromagnético e propagação de ondas* (Clube de Autores, Curitiba, 2015).
[13] W.E.H. Lecky, *Democracy and liberty* (Longmans, Green and Company, London, 1896), v. 2.
[14] A. Atkeson and P.J. Kehoe, The transition to a new economy after the second industrial revolution (National Bureau of Economic Research Cambridge, Cambridge, 2001), v. 2.
[15] J. Al-Khalili, Phil. Trans. R. Soc. A **373**, 20140208 (2015).
[16] M. Faraday, Phil. Mag **11**, 300 (1832).
[17] J. Henry, *On the production of currents and sparks of electricity from magnetism* (American Journal of Science and Arts, Cambridge, 1832).
[18] G.S. Smith, European Journal of Physics **38**, 015207 (2016).
[19] W.M. Stine, Journal of the Franklin Institute **155**, 363 (1903).
[20] F.E. Neumann, Annalen der Physik **143**, 31 (1846).
[21] R. Hessel, A.A. Freschi and F.J.D. Santos, Revista Brasileira de Ensino de Física **37**, 1506 (2015).
[22] N.A. Lemos, *Convite à física matemática* (Editora Livraria da Física, São Paulo, 2013).
[23] P. Lorrain, D.R. Corson and F. Lorrain, *Electromagnetic Fields and Waves* (W.H. Freeman and Company, New York, 1988).
[24] A. Feoli, A.L. Iannella and E. Benedetto, Revista Brasileira de Ensino de Física **43**, e20210017 (2021).
[25] D. Koks, *Explorations in mathematical physics: the concepts behind an elegant language* (Springer, New York, 2006).
[26] M. Goto, Revista Brasileira de Ensino de Física **32**, 1310 (2010).

 DOI: https://doi.org/10.1590/1806-9126-RBEF-2023-0297